Author‘s Manuscript - Public Access

Max-Planck-Institut für Polymerforschung
Max Planck Institute for Polymer Research

This is the peer reviewed version of the following article:

Kuan, S. L., Wang, T., Raabe, M., Liu, W., Lamla, M., & Weil, T. (2015). Programming Bioactive Architectures with Cyclic Peptide Amphiphiles. *ChemPlusChem, 80*(8), 1347-1353. doi:10.1002/cplu.201500218.

, which has been published in final form at: 10.1002/cplu.201500218

Programming Bioactive Architectures with Cyclic Peptide Amphiphiles

Seah Ling Kuan, Tao Wang, Marco Raabe, Weina Liu, Markus Lamla, Tanja Weil

This article may be used for non-commercial purposes in accordance with publisher’s Terms and Conditions for Use of Self-Archived Versions

COMMUNICATION

Programming Bioactive Architectures via Cyclic Peptide Amphiphiles

Seah Ling Kuan,[#*1] Tao Wang, [# 1] Marco Raabe,[1] Weina Liu, [1] Markus Lamla,[1] Tanja Weil*[1]

To Singapore on the occasion of its 50th year of independence

Abstract: We present a versatile approach for the synthesis of cyclic peptide amphiphiles of the hormone somatostatin (SST) with tunable lipophilic tails to program bioactive nanoarchitectures. A novel bis-alkylation reagent is synthesized that allows for the functionalization of SST with a thiol anchor. Different hydrophobic moieties are introduced inspired by a biomimetic palmitoylation approach which opens access to cyclic peptide amphiphiles that display rich self-organization and cell membrane interactions.

The synthesis and design of peptide amphiphiles (PAs) has attracted considerable attention towards various applications in biotechnology and biomedicine including drug delivery and regenerative medicine.[1–5] Peptide derivatives with amphiphilic properties due to alternating sequences of hydrophobic and hydrophilic (charged) residues that assemble into higher order nanostructures have been reported.[6–8] Additionally, peptides that are modified through the attachment of hydrophobic lipid chains which have either displayed unique self-assembly properties or have been adopted as non-covalent anchors for insertion into nanocarriers such as liposomes.[9,10] In particular, the design of PAs with bioactive peptides such as targeting ligands is highly attractive for the directed delivery of drugs or bioimaging agents.[10] Although the library of synthetic linear PAs is abundant in the literature, examples of synthetic cyclic PAs still remain scarce.[11–13]

Cyclic peptides play important roles in many cellular processes including cellular signaling. Moreover, they are known to be more stable and usually exhibit higher target-binding affinity compared to the corresponding linear counterparts due to their rigid scaffolds.[14] Cyclic lipopeptides comprising of a cyclic peptide headgroup with a lipid tail are expressed by bacteria and possess a rich pharmacology with antibacterial, antifungal and antiviral activities.[15] Consequently, the functionalization of bioactive cyclic peptides that introduces new features for controlling bioactivity or self-assembly[13,16–20] could be valuable for many therapeutic applications.

Still, the site-directed attachment of hydrophobic moieties such as lipids to cyclic peptides and subsequent purification are challenging to achieve. [21,22] One of the few examples is the well-known cyclic RGDFK PA; it contains a di-alkyl lipid chain attached to the cyclic peptide through the lysine ε-amino group.[23] This elegant approach only requires the presence of a single lysine residue that is not involved in the bioactivity of the peptide. Therefore, larger cyclic peptides with multiple lysines located in or close to the protein binding site cannot be modified by this reaction. As a result, there is a considerable interest in developing a synthetic PA platform containing a more versatile chemical approach.

In the cellular machinery, post-translation processes allow for the modification of proteins with lipids and one of the predominant modifications occurs via the free cysteine residue.[24] In this aspect, the physiological palmitoylation machinery could serve as a good synthetic model for deriving amphiphilic cyclic peptides in a site-directed manner. Theoretical evaluation of protein databases shows that most therapeutically relevant polypeptides and proteins offer at least one disulfide bond that is close to the surface that is directed away from the active sites. [25] Many cyclic peptides found in Nature such as somatostatin or oxytocin possess a single disulfide bridge that imparts stability and is often crucial for adopting the correct bioactive 3D architecture. [26,27] However, the presence of disulfide bridges in cyclic peptides often limits the possibilities to introduce additional free cysteine residues due to disulfide scrambling that leads to wrongly folded non-active peptides and thus reduces the yields during peptide expression or solid phase synthesis.[28,29]

Herein, we report the the synthesis of three cyclic PAs of the peptide hormone somatostatin (SST) whose amphiphilic properties are tuned in a versatile manner to tailor different bionanoarchitectures. SST is a neuropeptide that is efficiently uptaken into cells and translocated into the cytosol. This is mediated via five G protein-coupled membrane bound receptors (SSTR1 - 5) that are overexpressed in several tumors including breast, lung, prostate and neuroendocrine cancers.[30–32] SST derivatives can serve both as targeting ligands as well as antiproliferative drugs.[33,34] Due to their bioactivities, SST conjugates are of immense clinical interest for radiotherapy, tumor imaging and chemotherapy.[35,36]

The functionalization of SST is based on the structural novel bis-alkylation reagent, 2-((*tert*-butoxycarbonyl)thio)ethyl 2-(tosylmethyl)acrylate (**3**) that introduces a single thiol anchor group by converting the chemically labile disulfide bond into two more stable bissulfides (Scheme 1). Bis-alkylation reagents have been used for the functionalization of peptide hormones,[37–39] antibodies,[25,40] oligonucleotides[41] and therapeutic proteins.[40] In contrast to conventional bissulfone reagents containing three phenyl rings,[37] **3** offers improved solubility and imparts the thiol anchor in aqueous conditions allowing for various post-modifications with hydrophobic substituents. (Scheme 1a).[42]

The bis-alkylation reagent **3** was synthesized via a multistep reaction sequence (Scheme 1b, Supplementary information (SI)). *O*-(*tert*-butyl) *S*-(2-hydroxyethyl) carbonothioate (**1**) was first

[1] Dr. S. L. Kuan, Dr. T. Wang, Mr. M. Raabe, Ms. W. Liu, Dr. M. Lamla, Prof. Dr. Tanja Weil
Institute of Organic Chemistry III – Macromolecular Chemistry & Biomaterials, Ulm University
Albert-Einstein-Allee 1, 89081 Ulm Germany
E-mail: tanja.weil@uni-ulm.de
seah-ling.kuan@uni-ulm.de
#Shared 1st authorship
Supporting information for this article is given via a link at the end of the document.

UNDER

synthesized in 85% yield to protect the thiol group for subsequent reactions. Thereafter, it underwent a reaction with methacryloyl chloride to afford 2-((*tert*-butoxycarbonyl)thio)ethyl methacrylate (**2**) in 83 % yield. Finally, **3** was derived in 59 % yield from the oxidation of **2** and sodium *p*-toluene sulfinate. Compound **3** contains a mono-sulfone group as the reactive species and can react with SST via two consecutive Michael additions in aqueous buffer.[42]

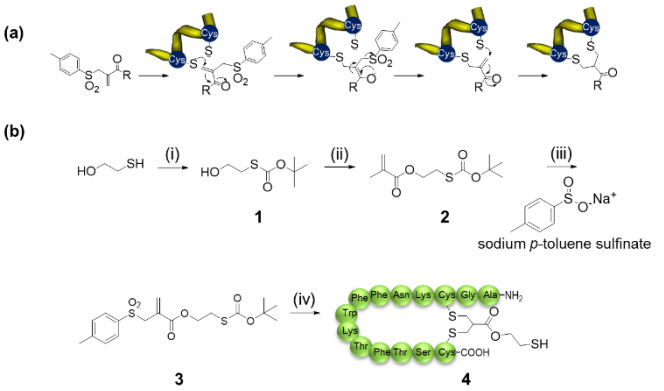

Scheme 1. Synthesis of SH-SST **4**. (i) K_2CO_3, Boc_2O, ACN, 24h, 85 %; (ii) Et_3N, methacryloyl chloride, anhydrous DCM, overnight, 83 %; (iii) I_2, sodium p-toluene sulfinate, DCM, 3d, then 3 eq. Et_3N RT overnight and reflux overnight in EA, 59 %; (iv) SST, TCEP, 50 mM PB, pH 7.8, 24 h, then TFA/MiliQ H_2O (2:1), 1h, 41 %.

The disulfide of SST was first reduced by tris(2-carboxyethyl)phosphine hydrochloride (TCEP) in 50 mM phosphate buffer (PB) at pH 7.8 and then incubated with **3** overnight at room temperature. We postulated that **3** reacted with a free thiol group of the reduced disulfide, followed by the subsequent elimination of the *p*-toluenesulfinic acid group to form a second Michael system. In the presence of another thiol group in close vicinity, the second Michael addition occurred with the concomitant formation of a C3-rebridged bissulfide.[40] The product was purified via HPLC, followed by Boc-deprotection in TFA/H_2O (2:1) for 1 h at room temperature to afford the thiol-functionalized SST, SST-SH (**4**) in 41 % yield over two steps. There is almost an two-fold increase in the yield of SST-SH by applying this method as compared to the strategy of using conventional bissulfone reagent that we have reported previously [37] due to the improved solubility of the bis-alkylation reagent in aqueous medium.

Thiol-maleimide chemistry is often employed in bioconjugation reactions due to fast reaction kinetics, atom efficiency, catalyst-free conditions and the improved stability of the thioether addition product.[43,44] Thus, it is attractive to apply thiol-maleimide chemistry to program the amphilicity of cyclic peptides through a thiol anchor. Hydrophobic maleimide groups **6**-**8** were prepared via the reaction of N-(2-aminoethyl) maleimide trifluoroacetate salt (**5**) with either the NHS esters (**Py-NHS**, **Pal-NHS**) or the acid chloride (**Cho-Cl**) as depicted in scheme 2a in moderate to high yield (63-81 %). The hydrophobic groups were selected for their different functions and lipophilicities, as determined from the calculated values of the octanol/water partition coefficients (log P(o/w)), with increasing hydrophobic character in the following order: pyrene < palmitoyl < cholesteryl groups (Table 1). Pyrene also reveals interesting photophysical properties due to the long lifetime of its monomers and its efficient formation of excimers,[45] that can provide a fluorescence probe for additional characterization, as well as the possibility to interact with hydrophobic drugs through Π-Π interactions for host-guest encapsulation. The two lipids cholesterol and palmitic acid are essential components in mammalian cell membranes and facilitate insertion of bioactive peptide amphiphiles into nanocarriers such as liposomes or carrier proteins in a non-covalent fashion.[9,10] The resultant bioactive amphiphiles had been exploited as targeting ligands to modulate transport across biological barriers and the localization of the carrier inside tumor cells.[46]

Table 1. log P(o/w) values obtained for SST and compounds **4**-**8**.

SST	**6**	**7**	**8**
-3.01	4.29	6.97	5.23
SST-SH (4)	**9a**	**9b**	**9c**
-3.24	0.43 (18.7)[a]	3.11 (20.1)[a]	1.36 (19.7)[a]

[a]HPLC retention time in mins

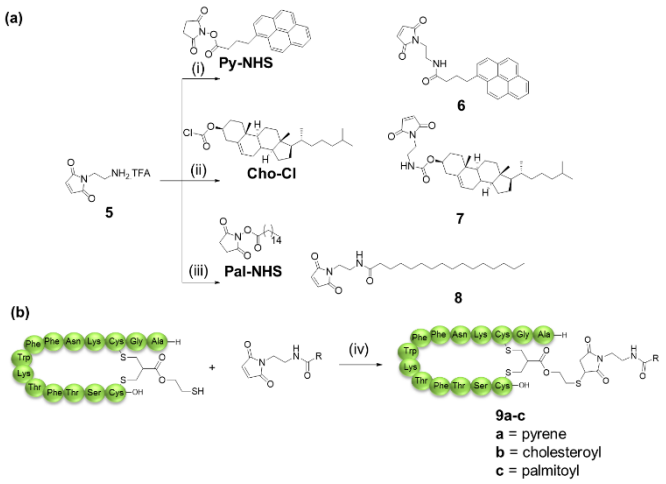

Scheme 2. (a) Synthetic scheme of hydrophobic maleimide units **6**-**8**: (i) pyrene-N-hydroxysuccinimide ester (**Py-NHS**), DIEA, DMF, RT, overnight, 81 %; (ii) cholesteryl chloroformate (**Cho-Cl**), DIEA, DMF/$CHCl_3$, RT, overnight, 63 %; (iii) palmitic acid N-hydroxysuccinimide ester (**Pal-NHS**), DIEA, DMF/$CHCl_3$, RT, overnight, 70 %. (b) Synthesis of somatostatin amphiphiles **9a**-**c** via biomimetic approach: (iv) maleimides **6**-**8**, DMF/$CHCl_3$, 48 h (56 %, 23 %, 69 %, respectively.

The reaction of **4** with the respective hydrophobic maleimides (**6**-**8**) was carried out under argon atmosphere in dimethylformamide (DMF)/chloroform ($CHCl_3$) over 48 h to afford amphiphilic somatostatin analogues **9a**-**c** as shown in scheme 2b. **9a** was obtained in 56 % yield after purification and MALDI-ToF MS is in agreement with mass signals at 2194.92 $[M+H]^+$ (SI, Figure S4). Successful conjugation of pyrene in **9a** was further corroborated by the characteristic absorption of pyrene at 346 nm and its fluorescence emission spectrum (SI, Figure S5). Excimer formation of **9a** was observed at 0.25 wt % (2.5 mg/mL). **9b** and **9c** were obtained in *ca*. 23 % and 69 % yields respectively, and

were identified by MALDI-ToF MS (**9b**: 2337.14 $[M+H]^+$; **9c**: 2163.04 $[M+H]^+$).The calculated log P(o/w) values (Table 1) corroborate with the HPLC retention times of the cyclic PAs and indicate that the hydrophobic character of the cyclic amphiphiles is strongly influenced by the hydrophobic units, increasing in the order: pyrene < palmitoyl < cholesteryl groups.

It had been demonstrated that SST conjugates prepared using a similar bis-alkylation scheme act as potent SSTR2 agonists and that they are internalized into MCF-7 cells which overexpress the SST receptors.[38] Thus, nanostructure formation with the SST PAs on the exterior could be important for therapeutic applications given the epitope's known bioactivity and was therefore further investigated. TEM images of **9a** at 0.5 wt % and 1 wt % showed that the formation of spherical assemblies have more homogenous size distribution at 1 wt % with an average diameter of 265 ± 40 nm (Figure 1a-b, SI, Figure S10). The pyrene residue in **9a** is expected to localize within the hydrophobic compartment of the spherical assembly and interact with aromatic hydrophobic dyes such as Nile Red (NR). Following a literature protocol for encapsulation studies,[47] **9a** was then mixed with NR in a 1:1 mole ratio to form **9a⊃NR**. The NR fluorescence lifetime has been reported to decrease significantly with an increase in the hydrogen-bonding capability of the solvent.[45,48] At 0.25 wt %, there was a sharp increase in fluorescence intensity upon the formation of the spherical assemblies that indicates the presence of NR within the hydrophobic compartments of the amphiphilic nanostructures (Figure 1c). In addition, a concomitant blue shift of the fluorescence emission (660 nm to 650 nm) and a nonradiative energy transfer (NRET) from the pyrene excimer to NR (Figure 1d) at λ_{ex} =346 nm were also observed, indicating the close proximity of **9a** and NR which is a result of the encapsulation of NR in the hydrophobic compartments of the spherical assemblies. The lipophilic tails of **9b** and **9c** can be employed as non-covalent anchors to arrange SST on the exterior of defined 3D architectures of nanocarriers in order to direct and modulate their localization in cells. We have chosen human serum albumin (HSA) as the carrier core for the proposed system based on its biocompatibility. HSA is a natural transporter for various molecules and one of the most exploited proteins used as a drug delivery vehicle in therapeutics and clinical biochemistry.[49–53] It is known to be involved in transport and storage in biological processes and possesses hydrophobic binding pockets for both exogenous and endogenous ligands.[50,54] It has seven binding sites for fatty acids (Figure 2a)[55] and cholesterol has been shown to bind to HSA with K_b value in the order of 10^5.[54] This unique feature of HSA to bind hydrophobic molecules has been exploited clinically: ABRAXANE®, an albumin-bound form of the anti-tumor drug paclitaxel, is currently available on the market as a drug for breast cancer treatment.[56] The combination of HSA with tumor-targeting groups and drugs is therefore highly promising for designing efficient translational drug transporter.[49]

Compounds **9b** and **9c** were applied as non-covalent anchors that assembled SST at the periphery of HSA via the interaction of the lipid or cholesterol substituents with the protein's binding pockets (Figure 2b). An excess of **9b** or **9c** was added to fluorescein-labelled HSA and incubated for 3 h. Thereafter, any unbound **9b** and **9c** were removed through ultrafiltration (MWCO = 30 kDa) to afford the SST loaded HSA analogues, **9b-HSA** and **9c-HSA**. Figure 2c shows the absorbance spectra of **9b-HSA**, **9c-HSA** and HSA with their concentration normalized using the absorbance signal of fluorescein at 480 nm. The absorbance values at 280 nm for **9b-HSA** and **9c-HSA** are much higher than native HSA due to the additional contribution of aromatic amino acid residues from somatostatin. This supports the successful binding of **9b** and **9c** to HSA. This was further substantiated by agarose gel electrophoresis where a new band appeared for **9b-HSA** with lower mobility (SI, Figure S12b) due to the increase in molecular weight and decrease in negative charge upon successful binding of the electropositive **9b** to HSA. The sizes of **9b-HSA** and **9c-HSA** as determined by dynamic light scattering (DLS) are 7.9±1.1 nm and 6.4±0.2 nm respectively (SI, Table S1). The slight increase in size compared to native HSA (6.3±1.0 nm) is presumably due to the binding of the somatostatin amphiphiles. AFM study of **9c-HSA** shows single macromolecules with a height of 1.5±0.4 nm comparable to HSA with a height of 1.4±0.4 nm (SI, Figure S13).

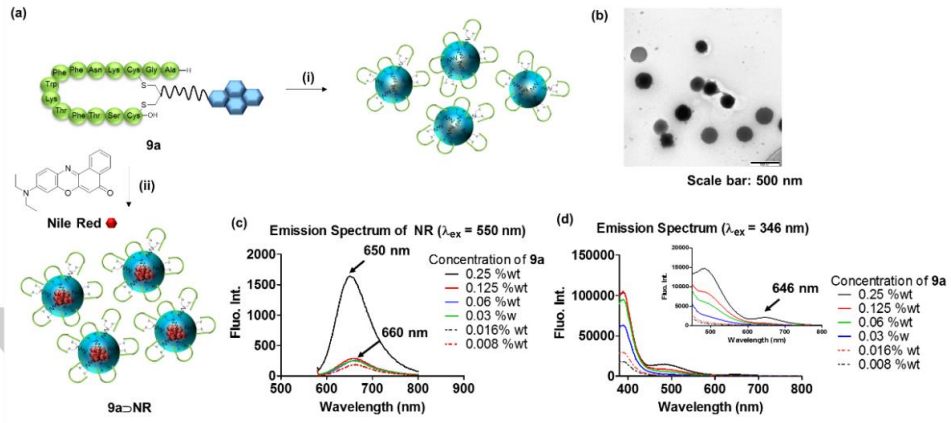

Figure 1. (a) Schematic representation of formation of spherical assemblies of **9a** and encapsulation of Nile Red (NR) dye. (i) 1 wt% **9a** in H_2O from a 5 wt% solution of **9a** in DMSO and (ii) 0.5 wt% **9a** and NR. (b) TEM image of 1 wt% **9a**. Sample is stained with 2 % sodium phosphotungstate adjusted to pH 7. (c) Emission spectra of NR incubated with varying wt% of **9a** showing incorporation of the hydrophobic dye at 0.25 wt%. (d) Emission spectra of NR incubated **9a**. Inset shows NRET from excimer of **9a** to NR at higher concentration.

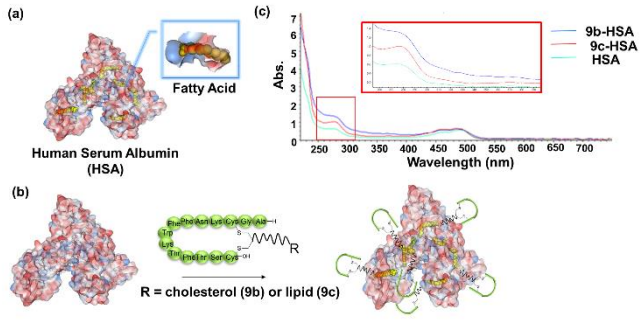

Figure 2. (a) Human serum albumin and its binding sites for fatty acids. (b) Binding **9b** and **9c** (10 mol. equiv.) to HSA (1 mol. equiv.). 3 h, RT. (c) Absorbance spectra of HSA, **9b-HSA**, **9c-HSA** showing successful binding. Inset depicts the expansion for absorbance at 280 nm. HSA used is fluorescein-labelled.

To investigate the bioactivity of the supramolecular SST towards SSTR positive cell lines after modification, a cellular uptake assay was accomplished in the human breast cancer cell line MCF-7 which expresses the SSTR2 receptor[33]. After 2 h of incubation with **9a** the fluorescence emission of lysed MCF-7 was obtained as an indicator for successful membrane translocation. A concentration dependent uptake of **9a** (Figure 3a) and the translocation of **9a⊃NR** across cellular membranes was also substantiated by confocal microscopy (Figure 3b).

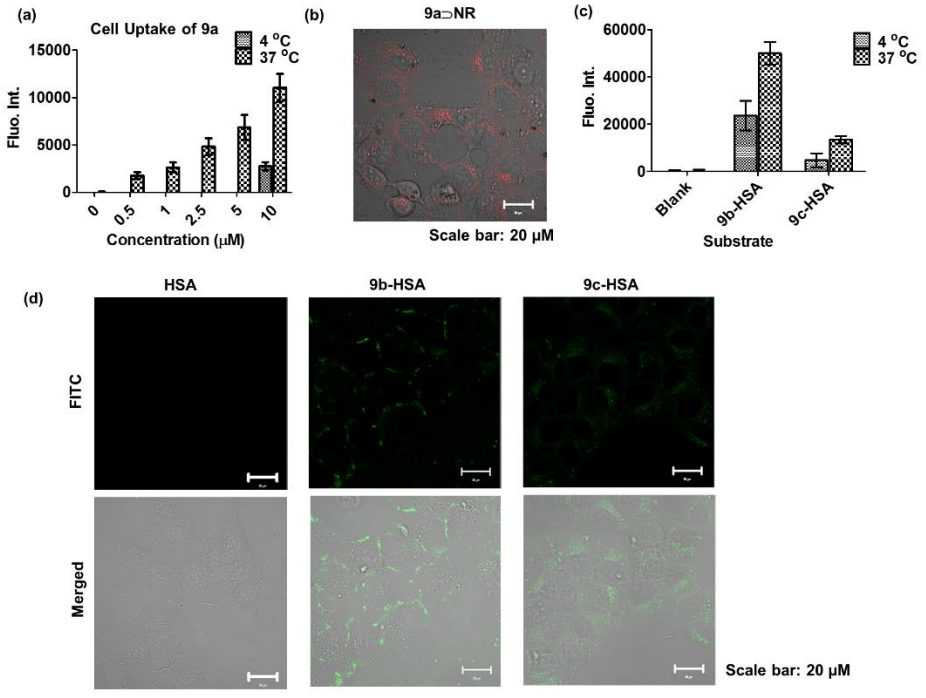

Figure 3. (a) Uptake of **9a** into MCF-7 cells, 2 h incubation, 37 °C. Comparison of uptake of **9a** into MCF-7 cells (10 μM) showed 75 % inhibition. (b) Confocal images of NR and **9a⊃NR** in MCF-7 cells, 4 h incubation. (c) Comparison of uptake of **9b-HSA** and **9c-HSA** (1 μM) into MCF-7 cells at 4 °C and 37 °C, 2 h incubation, with 53 % and 65 % inhibition, respectively. (d) Confocal images of NR and **9b-HSA**, **9c-HSA** and HSA in MCF-7 cells, 4 h incubation.

Next, we investigated the translocation of **9b-HSA** and **9c-HSA** across cellular membranes in comparison to native HSA, which does not permeate membranes of non-inflamed tissue.[57,58] It was observed that the cyclic PAs **9b** and **9c** facilitate the transport of fluorescein-labelled HSA into cells (Figure 3d). Interestingly, **9b-HSA** was localized in the cellular membranes while **9c-HSA** was internalized into the cells. The difference in the localization is presumably due to the cholesterol moiety in **9b-HSA** directing the anchored HSA to the cholesterol-enriched domains, which are known to be highly expressed in tumor cells.[59,60] Cell uptake studies of **9a**, **9b-HSA** and **9c-HSA** carried out at 4 °C and 37 °C were compared since receptor-mediated uptake is an energy-dependent process.[61] There is a significant inhibition of the cellular uptake of **9a**, **9b-HSA** and **9c-HSA** (Figure 3a, c) at 4 °C of 57 % (average over all concentrations), 53 % and 67 %, respectively (SI, Table S2-3), thereby clearly indicating that **9a**, **9b-HSA** and **9c-HSA** enter cells via receptor-mediated cell uptake rather than via passive diffusion.

Drawing inspiration from the cellular palmitoylation process, we have presented herein a two-step approach that allows the site-directed attachment of hydrophobic substituents in a convenient fashion in order to derive bioactive cyclic PAs through (1) the introduction of a thiol anchor to cyclic polypeptides and (2) capitalizing on the atom-efficient thiol-maleimide chemistry to achieve different lipid modifications. The peptide hormone SST was successfully functionalized with a thiol, and thus three different SST amphiphiles (**9a**-**9c**) were obtained from the SST-SH building block which complement the limited number of cyclic PAs in the literature. The SST amphiphiles were used to direct the assembly of different supramolecular bionanoarchitectures which could be used for drug delivery by encapsulating hydrophobic drugs with bioactive epitopes on the exterior as shown with **9a**. Or they could be employed to decorate the periphery of membrane impermeable proteins to facilitate their transport across cell membranes as shown with **9b** and **9c**. Notably, the SST amphiphiles **9a** and **9c** retain their SST bioactivity while the interaction of **9b** with cell membranes is seemingly dictated by the cholesterol group. Further investigation should be undertaken to evaluate the influence of the lipid residue on the subcellular localization of nanocarriers. Based on these studies, new strategies for the design of bionanomaterials that can be directed to various subcellular localizations for targeted drug transport could be evolved. One can envision that the chemical amphiphile approach presented herein represents a versatile platform with significant potential to chemically program various cyclic peptides via self-organization to direct drug molecules or imaging reagents to specific cellular

compartments in order to achieve efficient targeting at the subcellular level, which is of great interest in biomedicine and bioimaging.

Experimental Section

All experimental details and syntheses of compounds **1, 3**-**5** are available in the supplementary information.

Synthesis of SST-SH (4)

Somatostatin (SST, 40 mg, 24.4 µmol) was dissolved in 35 ml of phosphate buffer (PB, 50 mM, pH 7.8) and TCEP (14 mg, 48.8 µmol) in 1 ml PB (50 mM, pH 7.8) was added. To this solution, compound **3** (19 mg, 48.8 µmol) in 24 ml of ACN was added slowly. The resulting reaction mixture was incubated at RT for 24 h. The mixture was then concentrated and purified by Agilent 1260 HPLC using a LiChrospher® 100, RP-18, 10 µm, LiChroCART® 250-10 column with the mobile phase starting from 95 % solvent A (0.1 % TFA in water) and 5 % solvent B (0.1 % TFA in acetonitrile), raising to 30 % B at 5 min, further increasing to 80 % B at 10 min, reaching 95 % B at 22 min, keeping 95 % for 3 min , finally returning 5 % B at 30 min and balanced the column for 2 min with a flow rate of 4 ml/min. The absorbance was monitored at 280 nm and 220 nm. The product was dried from lyophilization and re-dissolved in 3 ml of TFA/MilliQ H_2O 2:1. The solution was stirred for 1 h at RT and 18 mg of the SH-SST **4** was obtained after lyophilisation in 41 % yield and characterized by MALDI-TOF-MS (m/z= 1783.7583 $[M+H]^+$). $C_{82}H_{114}N_{18}O_{21}S_3$. Calc. 1783.75915 $[M+H]^+$.

Synthesis of somatostatin amphiphiles (9a-c)

All manipulation and reactions were carried out under argon. To a solution of SST-SH (**4**) dissolved in anhyd. DMF at a concentration of *ca*. 1 mg/mL was added 10 mol. equiv. of the respective maleimides (**6**-**8**) dissolved in anhyd. DMF (**6**) or $CHCl_3$ (**7**-**8**) at a concentration of *ca*. 5 mg/mL and the reaction mixture was left to stir for 48 h at RT. The solvent was removed under reduced pressure and the solid was washed with 3 x 2 mL DCM to remove unreacted **6**-**8**. The resultant residue was then purified by HPLC to afford the **SST** amphiphiles (**9a**-**b**). All the products were characterized by MALDI-MS or LC-MS.

Pyrene-SST (9a). MALDI-ToF MS: MALDI-ToF MS: 2194.92010 $[M+H]^+$; ESI-MS: 1098 $[M+2H]^{2+}$ + H ; 731 $[M]^{3+}$. Chemical Formula: $C_{108}H_{136}N_{20}O_{24}S_3$ Exact Mass: 2193.9293 $[M+H]^+$.

Cholesterol-SST (9b). MALDI-ToF MS: 2337.14319 $[M+H]^+$; ESI-MS: 1169 $[M+2H]^{2+}$; 779 $[M]^{3+}$. Chemical Formula: $C_{116}H_{166}N_{20}O_{25}S_3$ Exact Mass: 2337.1432 $[M+H]^+$

Lipo-SST (9c). ESI-MS: 1082 $[M+ 2H]^{2+}$; 721 $[M]^{3+}$; MALDI-ToF MS: 2163.0415 $[M+ H]^+$;. Chemical Formula: $C_{116}H_{166}N_{20}O_{25}S_3$ [M] Exact Mass: = 2163.0052 $[M+H]^+$. HPLC purity: 81 %.

Transmission electron microscopy (TEM)

2 µL of 1 wt% or 0.5 wt% **9a** was added onto the holey carbon coated TEM grids, followed by washing with water to remove excess material and negatively stained with 2 wt% aqueous sodium phosphotungstate acid adjusted to pH 7. The TEM samples were air-dried overnight prior to imaging.

Encapsulation of Nile Red (NR) with 9a

1 µL of Nile Red (22.8 mM in $CHCl_3$:MeOH, 4:1) was mixed with 1 µL of **9a** (5 wt% in DMSO) and the volatile solvent was allowed to evaporate. Thereafter, water was added to a total volume of 10 µL (0.5 wt% **9a**) and the mixture was incubated for 30 mins at RT. The solution was diluted to 20 µL (0.25 wt% **9a**) for absorbance and fluorescent measurements. Six serial dilutions of **9a** were also made from 5 wt% to show the difference in encapsulation of NR. Fluorescence spectra were obtained at λ_{ex} = 346 nm and 550 nm.

Binding of 9b or 9c to human serum albumin

10 mol. equiv. of **9b** or **9c** was added to 0.5 mg of FITC-labelled HSA in water and the mixture was incubated for 3 h. Thereafter, excess **9b** and **9c** was removed via ultrafiltration three times against water using Vivaspin® 500 Centrifugal Concentrator (MWCO = 30 kDa). Protein concentration was determined by comparison of the absorbance at λ = 480 nm against a standard solution of FITC-labelled HSA (0.5 mg/mL).

Cell culture

MCF-7 cells, a human breast cancer cell line, were cultured in high-glucose DMEM supplemented with 10% fetal bovine serum (FBS), 100 U/mL penicillin, 0.1 mg/mL streptomycin, and 0.1 mM non-essential amino acids at 37°C in a humidified 5% CO_2 incubator. MCF-7 cells were plated into a white 96 well half area microplate at a density of 3000 cells (24 hr) per well in 50 µL complete DMEM and incubated overnight for attachment. For cell studies at 4ºC, the cells were preincubated for 30 mins at 4ºC before addition of substrates. Triplicates were obtained for all measurements.

Cell uptake

After cell attachment, **9a** (50 µL each of 0 µM, 1 µM, 2.5 µM, 5 µM, 10 µM), **9b-HSA** or **9c-HSA** (50 µL each of 1 µM) in fresh medium was applied to cells and was incubated for 2 h at 4 °C or 37ºC. The cells were then washed two times with ice-cold PBS (50 µL) to remove the non-internalized samples and lysed with 50 µL of lysis buffer (50 mM Tris, 0.8% Triton, 0.2% SDS, pH 7.4) and incubated at RT for 5 h. The cell uptake was determined from the fluorescence of the lysate using a TECAN Infinite M1000 microplate reader (**9a**: Ex 344 nm and Em 400 nm; **9b-HSA/9c-HSA**: Ex 488 nm and Em 520 nm).

Confocal Microscopy

MCF-7 cells were were plated in a Coverglass Lab-Tek 8-well chamber (Nunc, Denmark) at a density of 30,000 cells per well in 300 µl DMEM. The cells were incubated for overnight at 37 °C in 5% CO_2 to allow adhesion. Samples are prepared according to the description in ESI. Imaging was then performed using a LSM 710 laser scanning confocal microscope system (Zeiss, Germany) coupled to XL-LSM 710 S incubator and equipped with a 63× oil immersion objective. The acquired images were processed with Zen software developed by Carl Zeiss.

Acknowledgements

The authors are grateful to the financial support from the ERC Synergy Grant 319130-BioQ and the Volkswagen foundation, grant number Akz 86 366. We thank Stephan Fischer for the technical support and Andrew Norris and Adewola Osunsade for proofreading.

Keywords: Cyclic peptide amphiphiles, somatostatin, supramolecular albumin conjugates, protein bionanoarchitectures, targeting cellular compartments

[1] H. Cui, M. J. Webber, S. I. Stupp, *Pept. Sci.* **2010**, *94*, 1–18.
[2] N. Wiradharma, Y. W. Tong, Y. Y. Yang, *Macromol. Rapid Commun.* **2010**, *31*, 1212–1217.
[3] J.-X. Chen, H.-Y. Wang, C.-Y. Quan, X.-D. Xu, X.-Z. Zhang, R.-X. Zhuo, *Org. Biomol. Chem.* **2010**, *8*, 3142–3148.
[4] C. Valéry, F. Artzner, M. Paternostre, *Soft Matter* **2011**, *7*, 9583.
[5] D. Jiao, J. Geng, X. J. Loh, D. Das, T. C. Lee, O. A. Scherman, *Angew. Chem. Int. Ed.* **2012**, *51*, 9633–9637.
[6] C. C. Decandio, E. R. Silva, I. W. Hamley, V. Castelletto, M. S. Liberato, V. X. Oliveira, C. L. P. Oliveira, W. A. Alves, *Langmuir* **2015**, *31*, 4513–4523.
[7] X. D. Xu, C. S. Chen, B. Lu, S. X. Cheng, X. Z. Zhang, R. X. Zhuo, *J. Phys. Chem. B* **2010**, *114*, 2365–2372.
[8] I. W. Hamley, A. Dehsorkhi, V. Castelletto, *Langmuir* **2013**, *29*, 5050–5059.
[9] C.-W. Chen, D.-W. Lu, M.-K. Yeh, C.-Y. Shiau, C.-H. Chiang, *Int. J. Nanomedicine* **2011**, *6*, 2567–80.
[10] D. K. Chang, C. Y. Chiu, S. Y. Kuo, W. C. Lin, A. Lo, Y. P. Wang, P. C. Li, H. C. Wu, *J. Biol. Chem.* **2009**, *284*, 12905–12916.
[11] D. Oh, S. A. Darwish, A. N. Shirazi, R. K. Tiwari, K. Parang, *ChemMedChem* **2014**, *92618*, 2449–2453.

[12] S. Fernandez-Lopez, H. S. Kim, E. C. Choi, M. Delgado, J. R. Granja, A. Khasanov, K. Kraehenbuehl, G. Long, D. A. Weinberger, K. M. Wilcoxen, et al., *Nature* **2001**, *412*, 452–455.
[13] E. K. Chung, E. Lee, Y. B. Lim, M. Lee, *Chem. - A Eur. J.* **2010**, *16*, 5305–5309.
[14] E. M. Driggers, S. P. Hale, J. Lee, N. K. Terrett, *Nat. Rev. Drug Discov.* **2008**, *7*, 608–624.
[15] I. W. Hamley, *Chem. Commun.* **2015**, *51*, 8574–8583.
[16] Y. Loo, S. Zhang, C. A. E. Hauser, *Biotechnol. Adv.* **2012**, *30*, 593–603.
[17] A. R. Cormier, X. Pang, M. I. Zimmerman, H. X. Zhou, A. K. Paravastu, *ACS Nano* **2013**, *7*, 7562–7572.
[18] L. Li, H. Zhan, P. Duan, J. Liao, J. Quan, Y. Hu, Z. Chen, J. Zhu, M. Liu, Y. D. Wu, J. Deng, *Adv. Funct. Mater.* **2012**, *22*, 3051–3056.
[19] M. G. J. ten Cate, N. Severin, H. G. Boerner, *Macromolecules* **2006**, *39*, 7831–7838.
[20] R. J. Brea, C. Reiriz, J. R. Granja, *Chem. Soc. Rev.* **2010**, *39*, 1448–1456.
[21] J. T. Mika, G. Moiset, A. D. Cirac, L. Feliu, E. Bardají, M. Planas, D. Sengupta, S. J. Marrink, B. Poolman, *Biochim. Biophys. Acta - Biomembr.* **2011**, *1808*, 2197–2205.
[22] A. Clausell, F. Rabanal, M. Garcia-Subirats, M. a. Alsina, Y. Cajal, *Luminescence* **2005**, *20*, 117–123.
[23] V. Marchi-Artzner, B. Lorz, C. Gosse, L. Jullien, R. Merkel, H. Kessler, E. Sackmann, *Langmuir* **2003**, *19*, 835–841.
[24] M. J. Nadolski, M. E. Linder, *FEBS J.* **2007**, *274*, 5202–5210.
[25] S. Brocchini, A. Godwin, S. Balan, J.-W. Choi, M. Zloh, S. Shaunak, *Adv. Drug Deliv. Rev.* **2008**, *60*, 3–12.
[26] W. Tegge, W. Bautsch, R. Frank, *J. Pept. Sci.* **2007**, *13*, 693–699.
[27] A. Ortiz-Acevedo, G. R. Dieckmann, *Tetrahedron Lett.* **2004**, *45*, 6795–6798.
[28] H. T. He, R. N. Gürsoy, L. Kupczyk-Subotkowska, J. Tian, T. Williams, T. J. Siahaan, *J. Pharm. Sci.* **2006**, *95*, 2222–2234.
[29] L. Eldjarn, A. Pihl, *J. Am. Chem. Soc.* **1957**, *79*, 4589–4593.
[30] J. a Koenig, R. Kaur, I. Dodgeon, J. M. Edwardson, P. P. Humphrey, *Biochem. J.* **1998**, *336 Pt 2*, 291–298.
[31] R. Cescato, S. Schulz, B. Waser, V. Eltschinger, J. E. Rivier, H.-J. Wester, M. Culler, M. Ginj, Q. Liu, A. Schonbrunn, J. C. Reubi, *J. Nucl. Med.* **2006**, *47*, 502–511.
[32] E. J. Rolleman, P. P. M. Kooij, W. W. De Herder, R. Valkema, E. P. Krenning, M. De Jong, *Eur. J. Nucl. Med. Mol. Imaging* **2007**, *34*, 1854–1860.
[33] M. Volante, R. Rosas, E. Allìa, R. Granata, A. Baragli, G. Muccioli, M. Papotti, *Mol. Cell. Endocrinol.* **2008**, *286*, 219–229.
[34] G. Weckbecker, R. Liu, L. Tolcsvai, C. Bruns, *Cancer Res.* **1992**, *52*, 4973–4978.
[35] F. Barbieri, A. Bajetto, A. Pattarozzi, M. Gatti, R. Würth, S. Thellung, A. Corsaro, V. Villa, M. Nizzari, T. Florio, *Int. J. Pept.* **2013**, *2013*.
[36] C. Grötzinger, B. Wiedenmann, *Ann. N. Y. Acad. Sci.* **2004**, *1014*, 258–264.
[37] T. Wang, Y. Wu, S. L. Kuan, O. Dumele, M. Lamla, D. Y. W. Ng, M. Arzt, J. Thomas, M. J. O., B.-K. Christopher, T. Weil, *Chem. – A Eur. J.* **2015**, *21*, 228–238.
[38] T. Wang, D. Y. W. Ng, Y. Wu, J. Thomas, T. TamTran, T. Weil, *Chem. Commun.* **2014**, *50*, 1116–8.
[39] A. Pfisterer, K. Eisele, X. Chen, M. Wagner, K. Müllen, T. Weil, *Chem. – A Eur. J.* **2011**, *17*, 9697–9707.
[40] S. Shaunak, A. Godwin, J.-W. Choi, S. Balan, E. Pedone, D. Vijayarangam, S. Heidelberger, I. Teo, M. Zloh, S. Brocchini, *Nat. Chem. Biol.* **2006**, *2*, 312–313.
[41] T. Wang, A. Pfisterer, S. L. Kuan, Y. Wu, O. Dumele, M. Lamla, K. Muellen, T. Weil, K. Mullen, T. Weil, *Chem. Sci.* **2013**, *4*, 1889–1894.
[42] S. Brocchini, S. Balan, A. Godwin, J.-W. Choi, M. Zloh, S. Shaunak, *Nat. Protoc.* **2006**, *1*, 2241–2252.
[43] E. M. Sletten, C. R. Bertozzi, *Angew. Chem. Int. Ed.* **2009**, *48*, 6974–6998.
[44] B. D. Mather, K. Viswanathan, K. M. Miller, T. E. Long, *Prog. Polym. Sci.* **2006**, *31*, 487–531.
[45] G. Nizri, S. Magdassi, *J. Colloid Interface Sci.* **2005**, *291*, 169–174.
[46] I. Haralampiev, M. Mertens, R. Schwarzer, A. Herrmann, R. Volkmer, P. Wessig, P. Müller, *Angew. Chem. Int. Ed.* **2015**, *54*, 323–326.
[47] M. O. Guler, R. C. Claussen, S. I. Stupp, *J. Mater. Chem.* **2005**, *15*, 4507.
[48] S. Mukherjee, H. Raghuraman, A. Chattopadhyay, *Biochim. Biophys. Acta - Biomembr.* **2007**, *1768*, 59–66.
[49] B. Elsadek, F. Kratz, *J. Control. Release* **2011**, *157*, 4-28
[50] R. Hussain, G. Siligardi, *Int. J. Pept. Res. Ther.* **2006**, *12*, 311–315.
[51] Y. Li, K. Xiao, J. Luo, J. Lee, S. Pan, K. S. Lam, *J. Control. Release* **2010**, *144*, 314–323.
[52] S. L. Kuan, Y. Wu, T. Weil, *Macromol. Rapid Commun.* **2013**, *34*, 380–392.
[53] D. Y. W. Ng, Y. Wu, S. L. Kuan, T. Weil, *Acc. Chem. Res.* **2014**, *47*, 3471–3480.
[54] X. Tao, Q. Zhang, W. Yang, Q. Zhang, *Current Nanoscience* **2012**, 830–837.
[55] D. Charbonneau, M. Beauregard, H.-A. Tajmir-Riahi, *J. Phys. Chem. B* **2009**, *113*, 1777–1784.
[56] F. Kratz, *J Control Release* **2008**, *132*, 171–183.
[57] J. R. Levick, *Arthritis Rheum.* **1981**, *24*, 1550–1560.
[58] A. Wunder, U. Müller-Ladner, E. H. K. Stelzer, J. Funk, E. Neumann, G. Stehle, T. Pap, H. Sinn, S. Gay, C. Fiehn, *J. Immunol.* **2003**, *170*, 4793–4801.
[59] R. Tiwary, W. Yu, L. A. deGraffenried, B. G. Sanders, K. Kline, *Breast Cancer Res.* **2011**, *13*, R120.
[60] R. C. Allsopp, U. Lalo, R. J. Evans, *J. Biol. Chem.* **2010**, *285*, 32770–32777.
[61] D. Pesce, Y. Wu, A. Kolbe, T. Weil, A. Herrmann, *Biomaterials* **2013**, *34*, 4360–4367.

WILEY-VCH

Entry for the Table of Contents (Please choose one layout)

Layout 1:

COMMUNICATION

Cyclic peptide amphiphiles prepared via a bioinspired approach are employed to program various bioactive nanoarchitectures that display rich self-organization and cell membrane interactions.

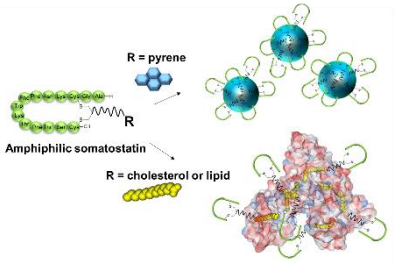

Seah Ling Kuan,[#] Tao Wang,[#] Marco Raabe, Weina Liu, Markus Lamla, Tanja Weil**

Page No. – Page No.

Title

Layout 2:

COMMUNICATION

((Insert TOC Graphic here))

*Author(s), Corresponding Author(s)**

Page No. – Page No.

Title

Text for Table of Contents

WILEY-VCH